Analysis of Lightning Characteristics and Hazard Prediction in Karimun Regency Using Maximum Entropy (MaxEnt) Modeling

Ilham Syarief Putra[1,2*], Lalu Muhamad Jaelani[2], and Muhamad Sawal[3]

[1]H.AS. Hanandjoeddin Class III Meteorological Station (BMKG), Tanjung Pandan 33411, Indonesia

[2]Department of Geomatics Engineering, Institut Teknologi Sepuluh Nopember, Surabaya 60111, Indonesia

[3]Raja Haji Abdullah Class IV Meteorological Station (BMKG), Tanjung Balai Karimun 29664, Indonesia

*ilham.putra@bmkg.go.id

Abstract: *This study analyzes the characteristics and predicts the lightning hazard zones in Karimun Regency, Indonesia, using the Maximum Entropy (MaxEnt) model. Lightning strike data from 2022 to 2024, consisting of 82,795 events, were analyzed along with environmental variables, including elevation, land cover, and rainfall. The MaxEnt model demonstrated good predictive performance with an Area Under the Curve (AUC) value of 0.654. Internal model analysis revealed that rainfall was the most influential variable in model formation, contributing 79.1%, followed by land cover (12.1%) and elevation (8.8%). Spatially, the distribution analysis showed that approximately 60% of lightning strikes occurred in lowland areas (0–22 meters above sea level), with shrub/vegetation areas experiencing the highest frequency. Interestingly, the statistical correlation between total monthly rainfall and lightning occurrences was consistently weak at all observation stations ($R^2 \approx 0$). Diurnally, lightning activity peaked in the afternoon (13:00–18:59). The final vulnerability map successfully identified high-risk areas concentrated in the subdistricts of Kundur, Kundur Utara, Kundur Barat, Buru, and Karimun. These findings provide valuable insights for lightning risk mitigation strategies, emphasizing that the complex interaction of various environmental factors drives lightning occurrence patterns in the tropical island region.*

Keywords: Elevation; Karimun Regency; Lightning Cover; Lightning Hazard; MaxEnt

Introduction

Across the globe, lightning stands out as a common and perilous weather occurrence, approximated to strike at an average rate of 44±5 times each second (Christian et al., 2003). This atmospheric electrical discharge occurs due to potential differences between clouds and the Earth's surface or between clouds themselves, causing significant economic losses and safety hazards worldwide (Rakov & Uman, 2001). Indonesia, as the world's largest archipelagic state, experiences substantial lightning frequency and ranks as one of the highest lightning activity regions globally, with Indonesia ranking 6th globally for total lightning events with over 81 million lightning events detected in 2021 (Vaisala, 2022).

Despite high lightning frequency in Indonesia, comprehensive spatial analysis and hazard prediction studies remain limited, particularly for small island regions. Traditional lightning risk assessment approaches often rely on simple statistical methods that may not adequately capture complex interactions between multiple environmental variables in tropical archipelagic environments. Karimun Regency, strategically located in the Riau Islands Province, represents a critical case study area with distinctive geographical characteristics. The region's complex topography, ranging from coastal lowlands to 444 meters elevation, combined with diverse land cover types across 12 sub-districts, creates an ideal setting for investigating lightning-environment relationships.

Previous studies have demonstrated that environmental factors such as topography, land cover, and precipitation patterns significantly influence lightning distribution. For example, research has detailed how storm charge structure, flash rates, and the spatial variability of lightning initiation vary with environmental conditions across U.S. regions (Fuchs et al., 2015; Fuchs & Rutledge, 2018) . Nonetheless, there are still certain limited geographic areas consisting of small islands, such as the Maritime Continent, that have not been investigated sufficiently. Studies into the characteristics of lightning in elevated terrains have revealed a tendency for more lightning strikes to occur per unit area as height above sea level increases (Pineda et al., 2007), but whether these continental patterns apply to small island environments requires investigation.

This research aims to fill a noticeable void in current scholarly work by utilizing Maximum Entropy (MaxEnt) modelling to chart the likelihood of lightning occurrences within a multifaceted tropical island setting. While MaxEnt is a well-established method for presence-only modelling in ecology (Elith et al., 2011; Phillips et al., 2006), its direct application to mapping lightning strike occurrence is uncommon in peer-reviewed literature. Previous related uses of MaxEnt include modelling lightning-ignited wildfire occurrence (e.g., Chen et al., 2015) , which shows the method's utility for lightning-related hazard problems but differs from direct strike-distribution mapping. By adapting MaxEnt to presence-only lightning observations and locally relevant environmental covariates, this study provides a novel regional application (Karimun Regency) that complements earlier studies on environmental controls of lightning (Fuchs et al., 2015; Fuchs & Rutledge, 2018) and lightning–precipitation relationships (Pineda et al., 2007).
The objectives of this study are: (1) to analyze the spatial and temporal characteristics of lightning in Karimun Regency for the 2022-2024 period, (2) to identify the environmental factors influencing lightning distribution, and (3) to develop a MaxEnt-based lightning hazard prediction model. The findings will contribute to lightning science by demonstrating

the effectiveness of machine learning for hazard prediction, while also supporting the development of early warning systems in tropical archipelagic regions.

Literature Review

Modern enhancements in the field of lightning tracking rely on the potential of expansive land-based grid systems, for instance, the National Lightning Detection Network in the United States, which offers ongoing, superior data for both climate studies and risk evaluation (Cummins & Murphy, 2009). Investigations into lightning patterns in tropical areas have taken advantage of information gathered by the Lightning Imaging Sensor (LIS) and Optical Transient Detector (OTD) to analyze how lightning events are spread out over time and space (Peterson et al., 2021). Explorations into the link between the amount of energy available for storms to form (CAPE) and how much lightning occurs have revealed significant connections between locations, offering a scientific rationale for why thunderstorms develop (E. Williams & Stanfill, 2002).

Lightning activity patterns have been extensively studied across different geographical regions, with particular emphasis on the role of topographic and land surface characteristics. Research conducted across different geographical areas has demonstrated that the physical features of the land have a considerable effect on where lightning strikes, showing a distinct trend where more lightning that connects clouds to the ground is seen as height above sea level increases (Bourscheidt et al., 2009). Yet, in areas near the coast or made up of islands, the connection between height and how often lightning occurs might change because of how the air moves near the sea and how differently land and water heat up.

The temporal distribution of lightning activity shows strong diurnal and seasonal patterns globally, with numerous studies documenting enhanced afternoon activity in tropical regions due to maximum surface heating and convective development (Albrecht et al., 2016; Christian et al., 2003; Peterson et al., 2021). Seasonal patterns are closely linked to regional monsoon cycles, with enhanced lightning activity during transitional periods when atmospheric instability is maximized.

Land cover type significantly influences lightning distribution through its effects on surface heating, moisture availability, and boundary layer development. Assessments conducted by scientists focusing on the link between atmospheric electricity and long-term weather trends reveal that the features of the ground, which are shaped by how land is utilized, give rise to very localized weather scenarios. These localized scenarios have the capacity to change the intensity of rising air currents (E. R. Williams, 2005). Agricultural areas and open vegetation often show higher lightning frequencies compared to dense forests or urban areas.

The relationship between precipitation and lightning occurrence has been a subject of extensive research, with studies showing varying correlations depending on regional climate characteristics and convective regimes. While heavy precipitation is often associated with thunderstorm activity, the relationship between rainfall and lightning varies across convective regimes. Tropical oceanic systems may produce large rainfall amounts with relatively few lightning flashes, whereas continental convective systems frequently generate intense lightning despite lower rainfall totals (Petersen & Rutledge, 1998). This complexity indicates that lightning occurrence is more closely linked to convective intensity than to total precipitation amounts.

Methodology

a. Study Area

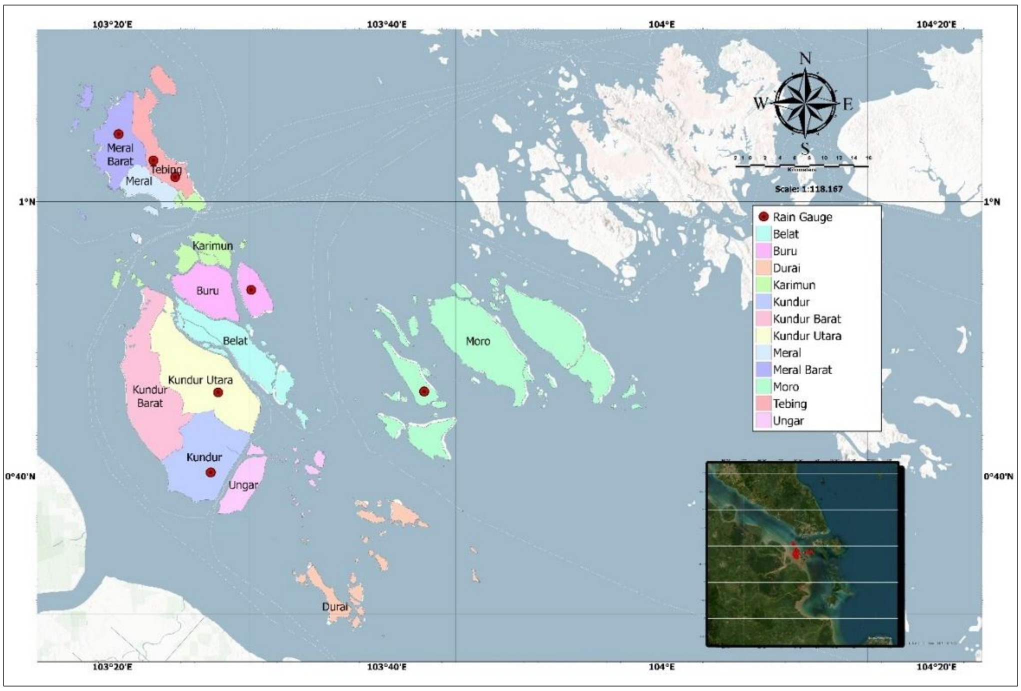

Figure 1: Study Area of Karimun Regency.

Karimun Regency is a governmental division situated within the Riau Islands Province of Indonesia. Tanjung Balai Karimun serves as the administrative center for Karimun Regency. The geographical coordinates of Karimun Regency span from 00° 24’ 36” North to 01° 13’ 12” North in latitude and from 103° 13’ 12” East to 104° 00’ 36” East in longitude, encompassing a marine zone that extends 4 nautical miles from its shores, as well as the Exclusive Economic Zone (EEZ), both of which are governed by Law Number 22 of 1999 and Law Number 05 of 1983.

b. Research Data

The data utilized in this study includes:

1. Information on Lightning: Data pertaining to lightning strikes gathered by the Lightning Detection Network sensor between 2022 and 2024, which includes details such as geographical coordinates, timestamps of when the strikes happened, and categorization of the lightning as either positive or negative Cloud-to-Ground strikes, or Intra-Cloud discharges. A total of 82,795 lightning events were recorded during the research period.
2. Precipitation Data: Monthly precipitation data from 6 rainfall observation stations (Buru, Kundur, Kundur Utara, Sememal, Stamet, and Tebing) for the period 2022-2024.
3. Data on Elevation: A Digital Elevation Model, or DEM, that offers a resolution of 30 meters, sourced from the Shuttle Radar Topography Mission, known as SRTM, classified into 5 classes: 0-22 m, 23-54 m, 55-107 m, 108-188 m, and 189-444 m.
4. Land Cover Data: Land cover map from 2022 based on Landsat 8 imagery interpretation, classified into 5 classes: water bodies, forest, settlement, paddy/agriculture, and shrubs/vegetation.

c. Data Analysis

1. Assessment of spatial and temporal variability: The investigation was carried out through the integration of documented lightning events alongside digital elevation models and land cover classifications, all processed within the ArcGIS software environment, specifically version 10.8. Temporal analysis included monthly distribution and diurnal patterns divided into 4 periods: According to the protocol used in studies examining worldwide lightning patterns, the timeframe is split into these categories: the initial hours of the day (from midnight to 5:59 AM), the period after sunrise until just before midday (6:00 AM to 12:59 PM), the time from early afternoon to just before sunset (1:00 PM to 6:59 PM), and the final hours of the day (7:00 PM to 11:59 PM).
2. Correlation assessment: The association between monthly rainfall totals and how often lightning occurred at different monitoring locations was determined using

Pearson's correlation method. The coefficient of determination (R^2) was used to assess the strength of relationships between variables, consistent with methodologies used in previous lightning-precipitation studies (Petersen & Rutledge, 1998).

3. MaxEnt Modeling: To forecast the geographical scattering of lightning risk, the MaxEnt software, version 3.4.1 (Phillips et al., 2006), was employed. A division of the lightning data allocated seventy-five percent for the training phase, with the remaining twenty-five percent reserved for validation purposes. The model's setup involved utilizing standard configurations, featuring 10,000 randomly selected background locations and capping the iterations at a maximum of 500. The assessment of the model's performance was carried out via ROC (Receiver Operating Characteristic) curves in conjunction with AUC (Area Under Curve) scores, consistent with recognized methodologies in species distribution modeling, but customized for lightning prediction (Phillips et al., 2006; Elith et al., 2010).

Results and Discussion

a. Spatial Distribution Analysis

Based on figure 2 the precipitation distribution map for the 2022-2024 observation period reveals significant spatial variation across all administrative areas of Karimun Regency. Precipitation values were divided into five classes based on quantile intervals: 21.014-95.481 mm (very low), 95.482-179.877 mm (low), 179.878-311.436 mm (medium), 311.437-485.193 mm (high), and 485.194-653.986 mm (very high). Areas with the highest precipitation were predominantly found in parts of Karimun, Buru, and western Meral sub-districts. This distribution indicates microclimate differences between islands, likely influenced by topographic orientation relative to wind direction, distance from open seas, and vegetation distribution patterns (Aldrian & Dwi Susanto, 2003).

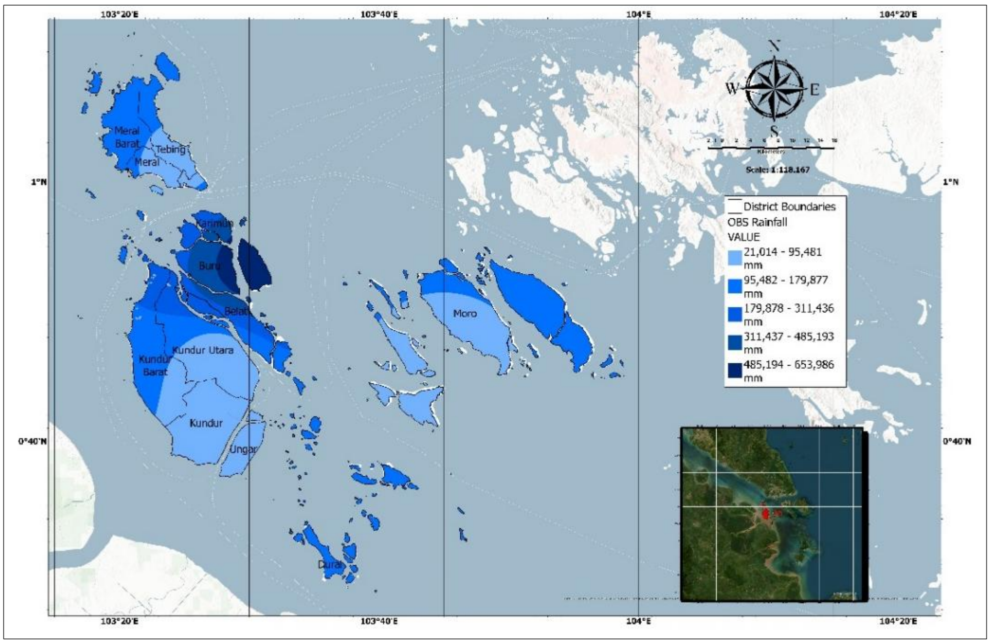

Figure 2: Precipitation Distribution Map of Karimun Regency (2022-2024).

The elevation map displays height variation above sea level across Karimun with classification based on height ranges in meters above sea level: 0-22 m (very low plains), 23-54 m (low plains), 55-107 m (gentle slopes), 108-188 m (medium hills), and 189-444 m (high hills) (Figure 3). Western Meral, parts of Tebing, and large islands like Moro and Durai exhibit high to very high elevations, reflecting significant hill presence. Most other areas, including Kundur Barat, Kundur Utara, Ungar, and Belat, are classified as lowlands.

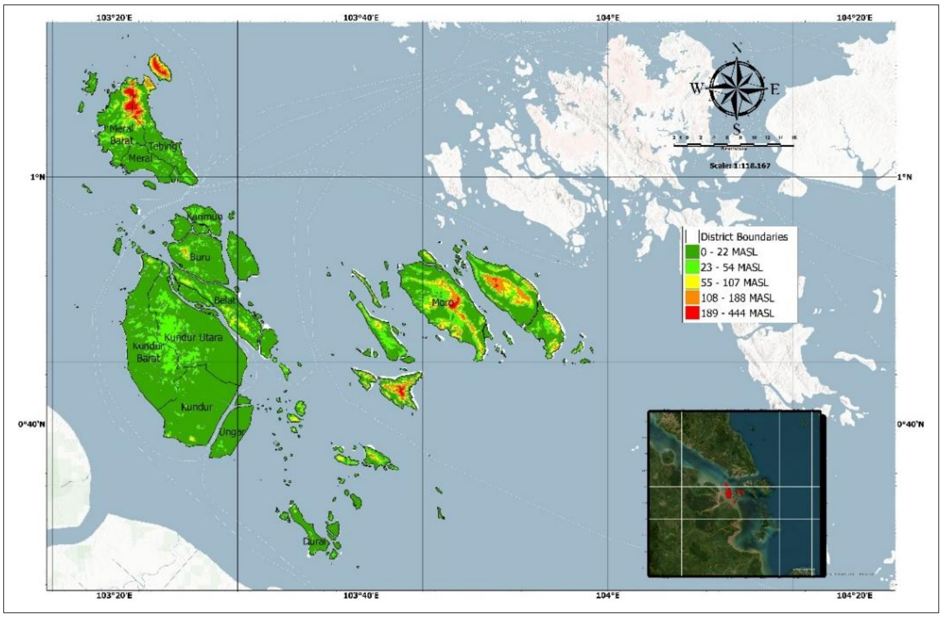

Figure 3: Elevation Map of Karimun Regency.

While in figure 4, the land cover map illustrates land use and coverage across Karimun, classified into five main categories: Water Body, Forest, Settlement, Paddy/Agriculture, and Shrubs/Vegetation. Settlements are concentrated in central activity areas such as Meral, Tebing, Karimun, and parts of Kundur Barat. Forest cover still dominates large islands like Kundur Utara, Moro, and Durai, indicating that parts of Karimun retain significant natural vegetation cover.

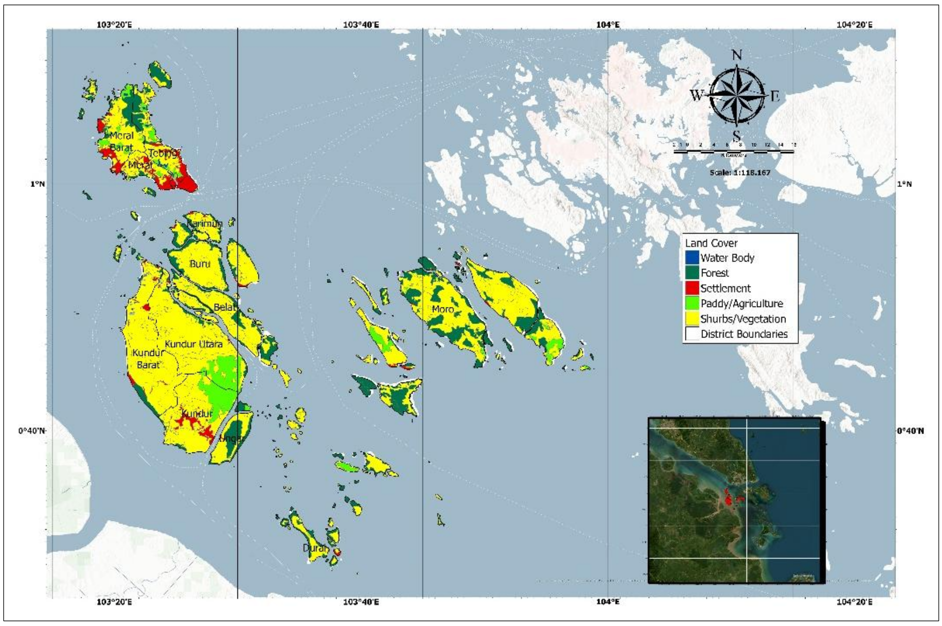

Figure 4: Land Cover Map of Karimun Regency.

b. Diurnal Lightning Pattern Analysis

The diurnal lightning pattern consistently showed peak occurrence during afternoon hours (13:00-18:59) across all observation years. The highest peak was recorded in 2023 with 11,001 strikes, followed by 2024 with 9,535 strikes and 2022 with 6,955 strikes. This phenomenon can be scientifically explained by maximum surface heating during daytime causing strong convection and Cumulonimbus cloud formation, which becomes the primary source of lightning strikes. This condition is characteristic of tropical regions like Karimun, surrounded by warm seas with high humidity (Mori et al., 2004).

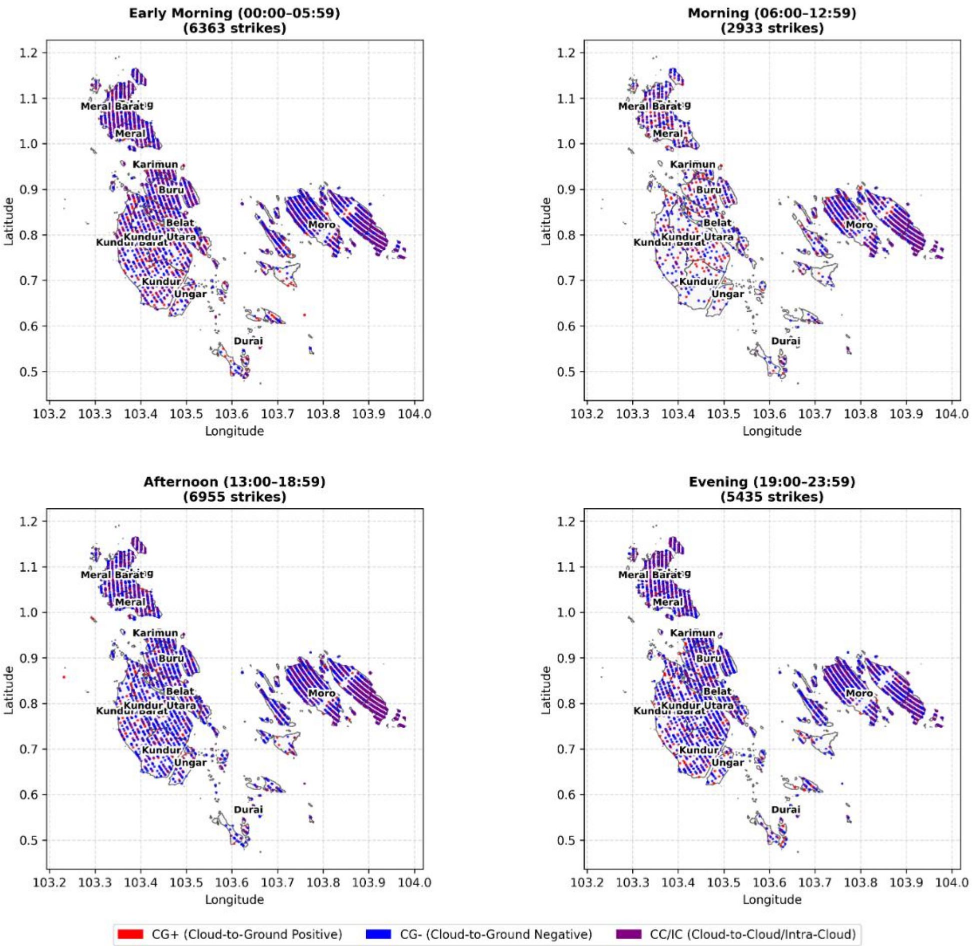

Figure 5: Diurnal Lightning Distribution in Karimun Regency for 2022.

Figure 5 presents the diurnal lightning distribution for 2022. The highest activity occurred in the Afternoon (13:00–18:59) with 6,955 strikes, dominated by CC/IC and CG– types, while CG+ occurred less frequently. Lightning strikes were concentrated across Meral Barat, Meral, Karimun, Tebing, Kundur, Kundur Utara, Kundur Barat, Ungar, Durai, and offshore waters near Moro. Other periods recorded 6,363 strikes (Early Morning), 5,435 (Evening), and 2,933 (Morning).

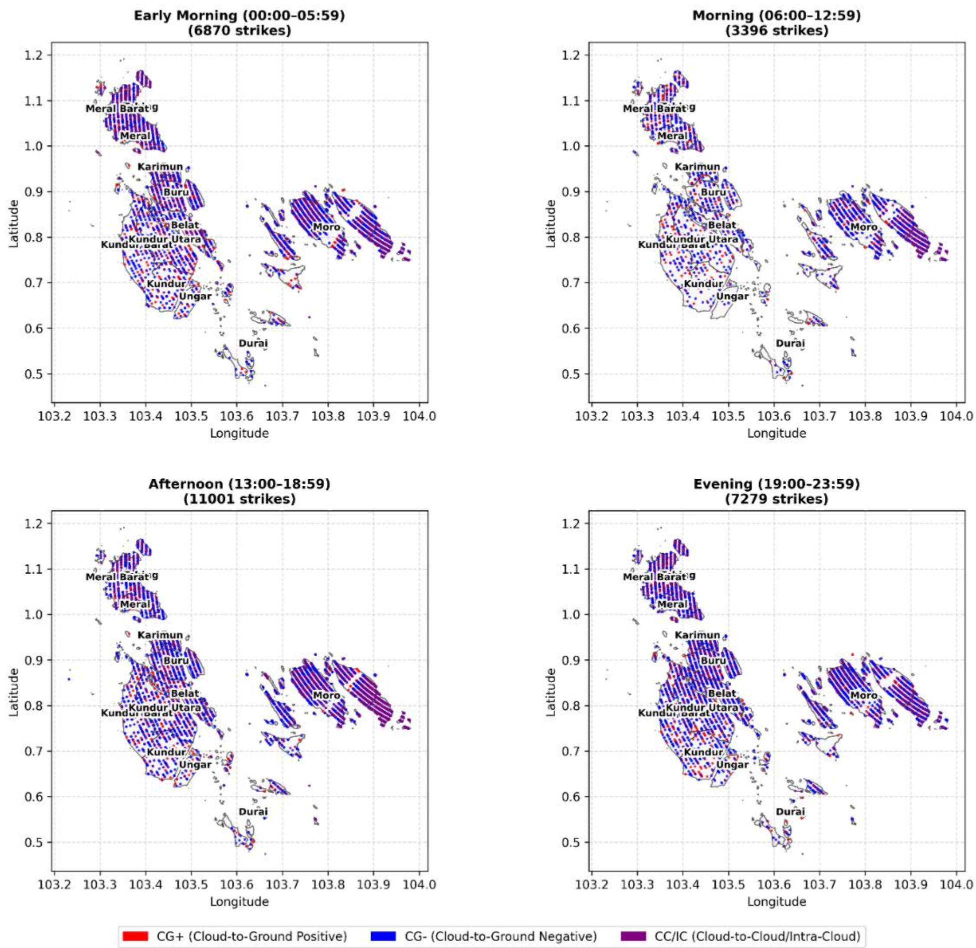

Figure 6: Diurnal Lightning Distribution in Karimun Regency for 2023.

Figure 6 shows the 2023 distribution, indicating a marked increase in lightning activity. Afternoon strikes reached 11,001, while Early Morning and Evening recorded 6,870 and 7,279 strikes, respectively, and Morning remained lowest at 3,396 strikes. Spatially, lightning concentrated in the same key districts Meral Barat, Meral, Karimun, Tebing, Kundur, Kundur Utara, Kundur Barat, Ungar, Durai, and coastal zones near Moro confirming persistent convective hotspots across both land and maritime areas.

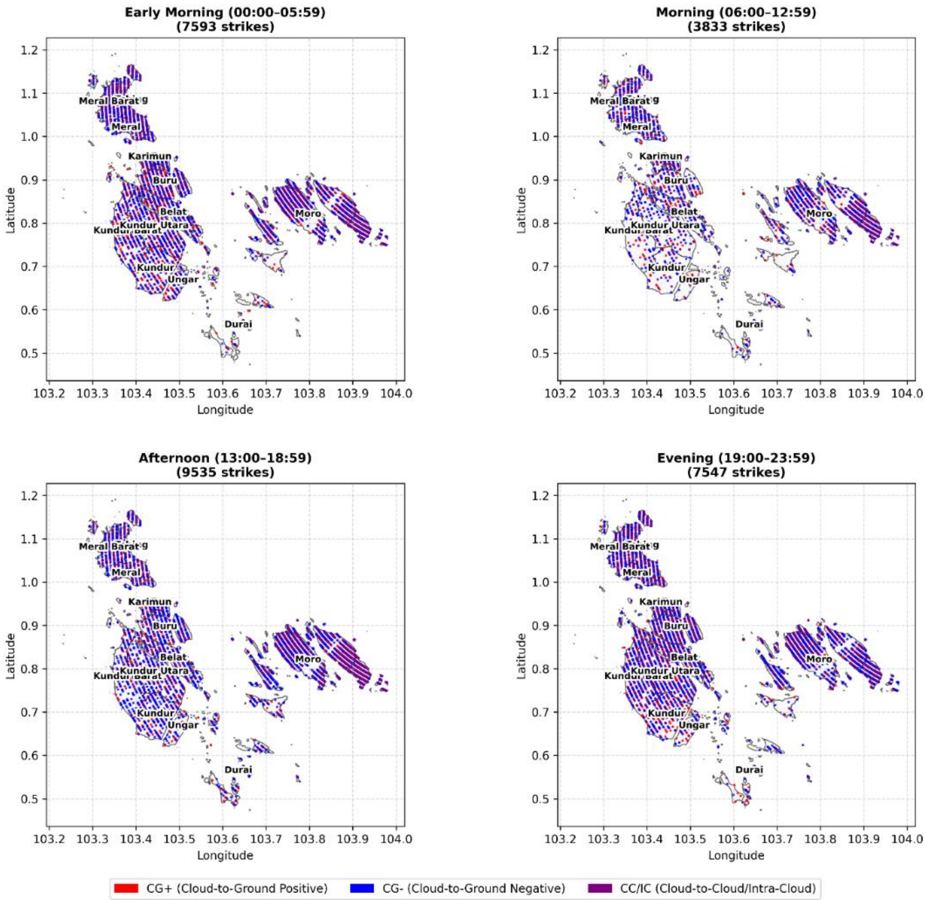

Figure 7: Diurnal Lightning Distribution in Karimun Regency for 2024.

Figure 7 illustrates the 2024 pattern, showing 9,535 strikes during Afternoon, 7,593 in Early Morning, 7,547 in Evening, and 3,833 in Morning. Strike distribution again followed the same spatial clusters, with Meral Barat, Meral, Karimun, Tebing, Kundur, Kundur Utara, Kundur Barat, Ungar, Durai, and Moro continuing as primary lightning-prone zones.

b. Lightning-Environment Relationships

Analysis of diurnal lightning distribution from 2022 to 2024 in Karimun Regency revealed consistent temporal patterns with peak lightning occurrence during afternoon to evening hours, influenced by convection dynamics from maximum heating. The regression analysis result, showing a negligible correlation between total monthly rainfall and lightning frequency (R2<0.02), is not a null result but rather a crucial finding that highlights a key nuance in tropical meteorology. This finding indicates that lightning activity is not tied to the accumulated volume of rain but is more closely related to the *convective intensity* of storms. Long-lasting stratiform rain can contribute to high total monthly rainfall without producing lightning, whereas short, intense convective storms produce abundant lightning with a possibly smaller contribution to the total monthly accumulation. Therefore, atmospheric instability metrics, such as CAPE, are likely more direct predictors of lightning activity than total rainfall (Petersen & Rutledge, 1998).

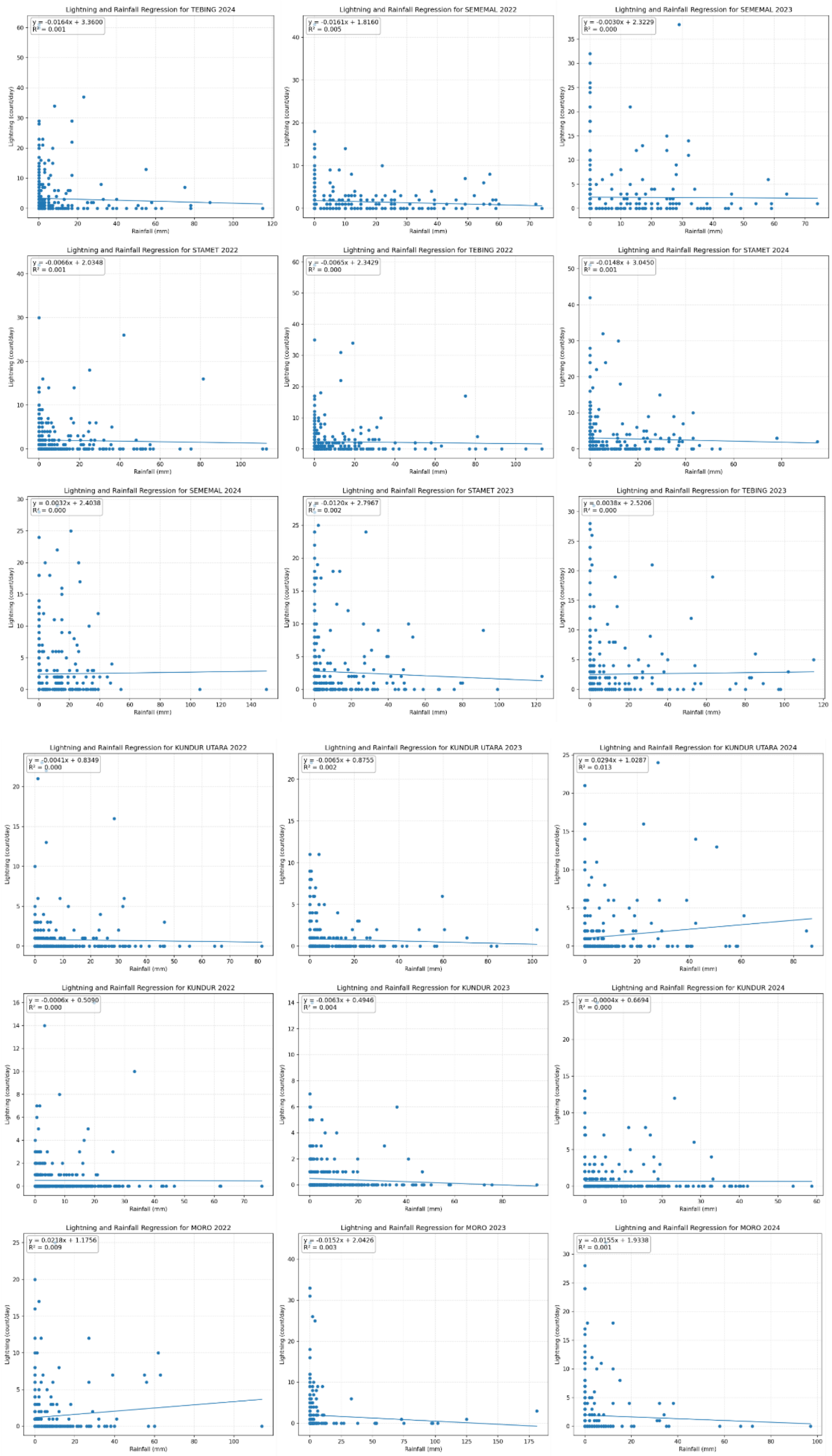

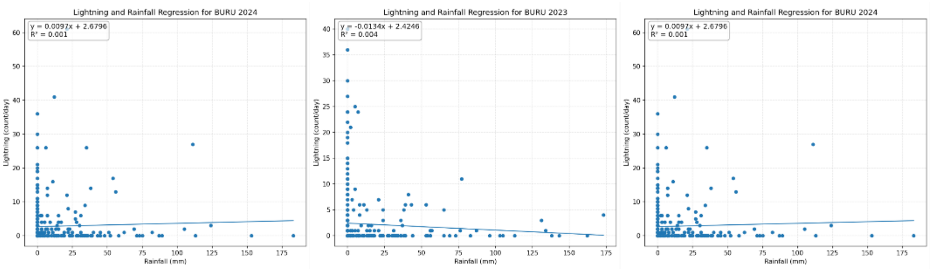

Figure 8: Precipitation vs Lightning Regression for 6 Rainfall Observation Stations.

Figure 8 shows across all stations and years (2022–2024), the daily scatterplots and fitted simple linear regressions show a consistently weak relation between rainfall and lightning. Coefficients of determination remain near zero across site–year pairs, and fitted slopes are small in magnitude, sometimes slightly positive and sometimes slightly negative. For illustration, Buru 2024 gives $y = 0.0097x + 2.6796$ with $R^2 = 0.001$, indicating that day-to-day changes in rainfall correspond to only negligible changes in lightning counts. The "strongest" case in the set, Kundur Utara 2024, is still weak ($y = 0.0294x + 1.029$, $R^2 = 0.0129$), and a negative example like Buru 2022 ($y = -0.0241x + 2.121$, $R^2 = 0.0117$) remains similarly uninformative. Visually, the point clouds are broadly dispersed around nearly flat regression lines, with many days containing zeros in one or both variables.

Annual summaries confirm that totals vary by station and by year—some sites show higher lightning counts in later years while annual rainfall modestly declines, whereas others remain relatively steady. However, these interannual differences do not translate into a clear daily linear association when examined within each location–year pair. In short, the figures and regression outputs consistently indicate that daily rainfall is not a reliable linear predictor of daily lightning at the stations considered during 2022–2024. These results are presented as obtained from the dataset, without further adjustments, and they are internally consistent across locations and years.

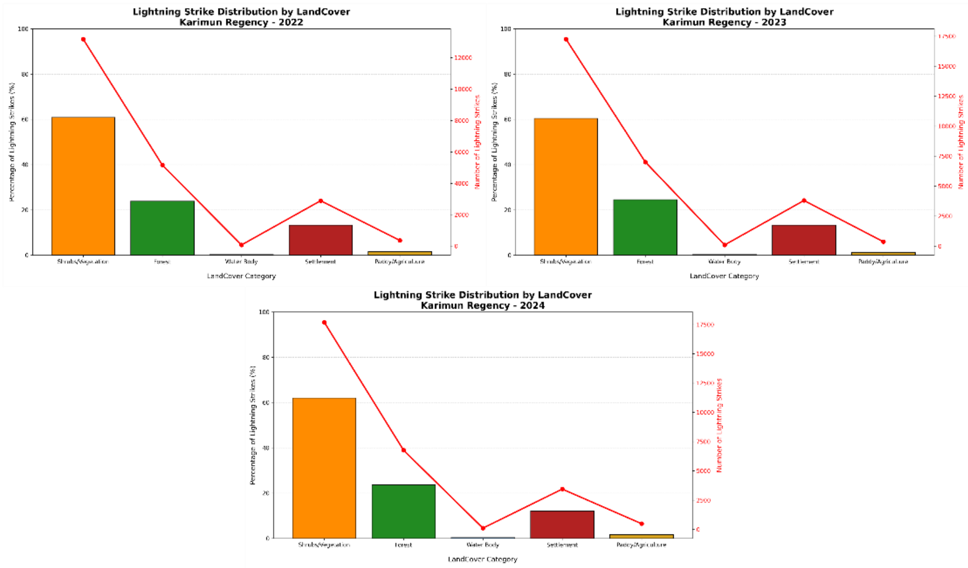

Figure 9: Lightning-Land Use Relationship.

Figure 9 shows that shrubs/vegetation and forest areas dominate lightning strike occurrences in Karimun Regency. Shrubs consistently account for about 65–70% of total strikes across 2022–2024, making them the primary land cover associated with lightning activity. Forests follow as the second major category, contributing around 20–25% of strikes. Settlements also register a smaller but notable proportion, approximately 8–12%, which indicates that built-up areas are not immune from lightning exposure. In contrast, paddy/agriculture land contributes less than 5%, and water bodies consistently record the lowest frequency, generally below 2% of strikes.

This pattern indicates that landscapes covered with plants, encompassing both bushes and wooded areas, are very important in influencing how often lightning happens. Their predominance could be attributed to surface properties such as roughness, evapotranspiration, and localized thermal effects that promote convective activity. The relatively low occurrence over water bodies reinforces the understanding that aquatic surfaces are less favorable for thunderstorm electrification.

These findings are consistent with studies from South America, where lightning density was shown to correlate strongly with both vegetated and deforested land covers. For example, research in Brazil highlighted that pasture/deforested areas as well as forests exhibited elevated lightning densities, likely due to their ability to retain moisture, alter surface roughness, and influence thermal gradients that drive convective processesb(Santos et al., 2024) .

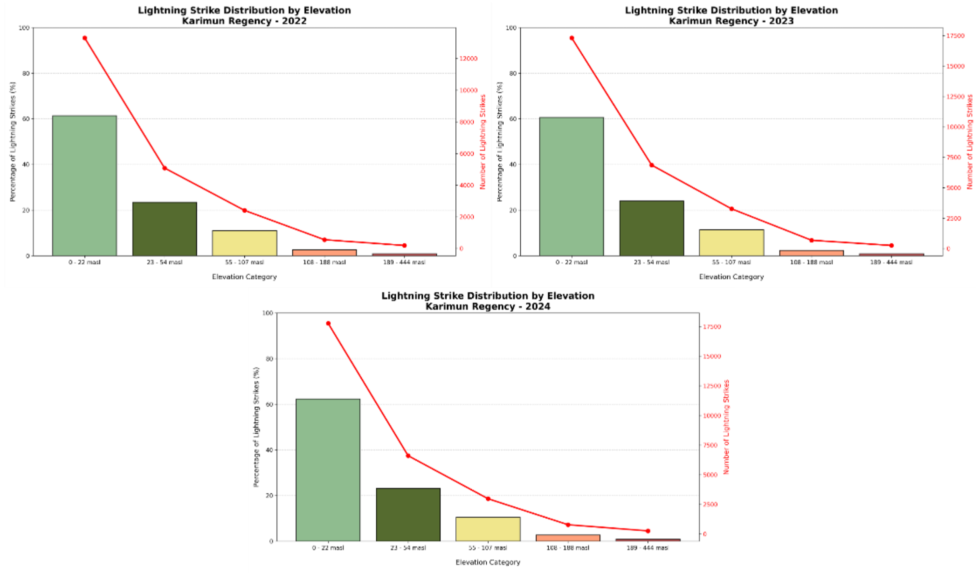

Figure 10: Lightning-Elevation Relationship.

Figure Figure 10 highlights the strong influence of elevation on lightning occurrence in Karimun Regency. The lowest elevation category 0–22 masl consistently registered the majority of lightning strikes, accounting for approximately 65–70% of the total across 2022–2024. The next elevation range 23–54 masl contributed about 20–25%, while areas between 55–100 masl recorded a much smaller share, roughly 7–10%. In contrast, higher terrains above 100 masl, including the 168–188 masl and 189–444 masl categories, showed very low frequencies, consistently below 5% of strikes.

This pattern demonstrates a clear decline in lightning occurrence with increasing altitude. Such results align with observations from tropical regions, where low-lying coastal plains are more favorable for lightning activity than elevated or mountainous terrain. Lower areas generally have higher atmospheric moisture content and are more exposed to localized heating from land–sea interactions, both of which enhance convective storm development. Comparable findings were reported in Sumatra, where lightning density was shown to correlate only weakly with elevation but more strongly with terrain slope. Specifically, the eastern lowlands exhibited higher lightning densities compared to the elevated Barisan Mountains (Yusnaini et al., 2021) . These results suggest that in addition to elevation, other geographic and land surface factors such as slope gradients, proximity to the coast, and land use patterns jointly modulate the spatial distribution of lightning strikes.

C. MaxEnt Modeling Analysis

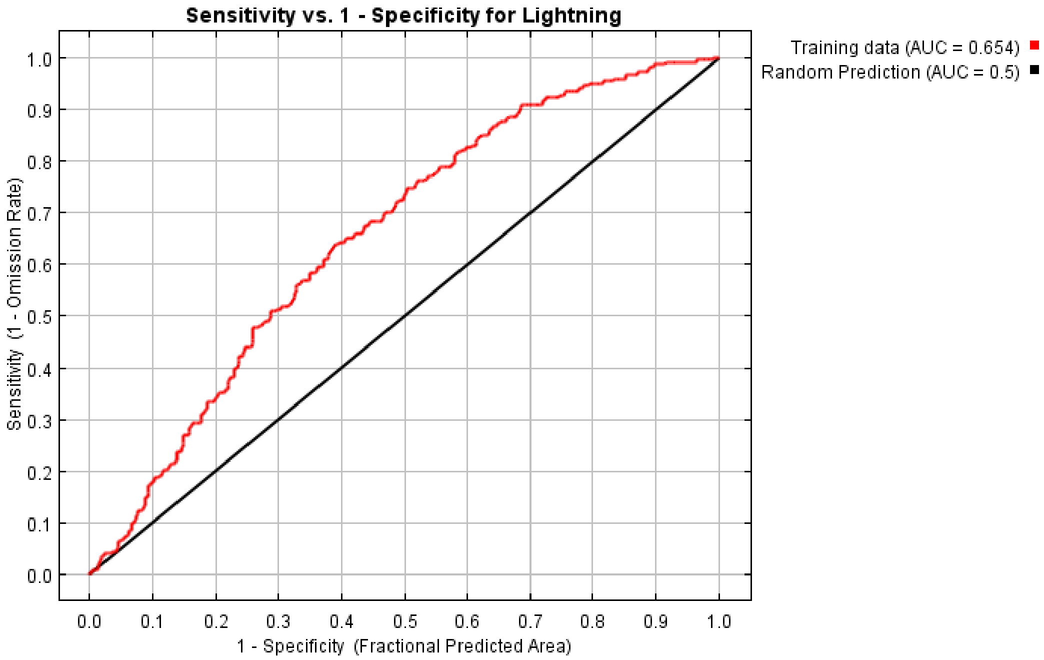

Source: Data Processing Results

Figure 11: ROC Curve of MaxEnt Model for Lightning Prediction.

As illustrated in Figure 11, the Receiver Operating Characteristic (ROC) curve was produced using the MaxEnt lightning prediction model. The model reached an AUC of 0.654, surpassing the random threshold of 0.5. Although the predictive ability is moderate, the result indicates that the model provides better performance than random guessing.

Given that lightning is an inherently stochastic and chaotic atmospheric process, the ability to obtain an AUC above 0.6 is already a meaningful achievement. It shows that the model is able to identify non-random patterns of occurrence. Importantly, the model relied only on static variables such as elevation and land cover, together with slow-varying environmental drivers like monthly rainfall, yet it still succeeded in capturing a predictive signal for an instantaneous event.

This result highlights the importance of underlying geographical and climatological factors in shaping lightning distributions. While the predictive capacity may be moderate, the model provides a valuable baseline that can be further improved by incorporating higher-resolution temporal variables such as atmospheric instability indices, convective available potential energy (CAPE), or real-time weather radar data. In this sense, the MaxEnt approach not only demonstrates its utility as an initial predictive framework but also opens opportunities for integrating more dynamic meteorological predictors in future studies.

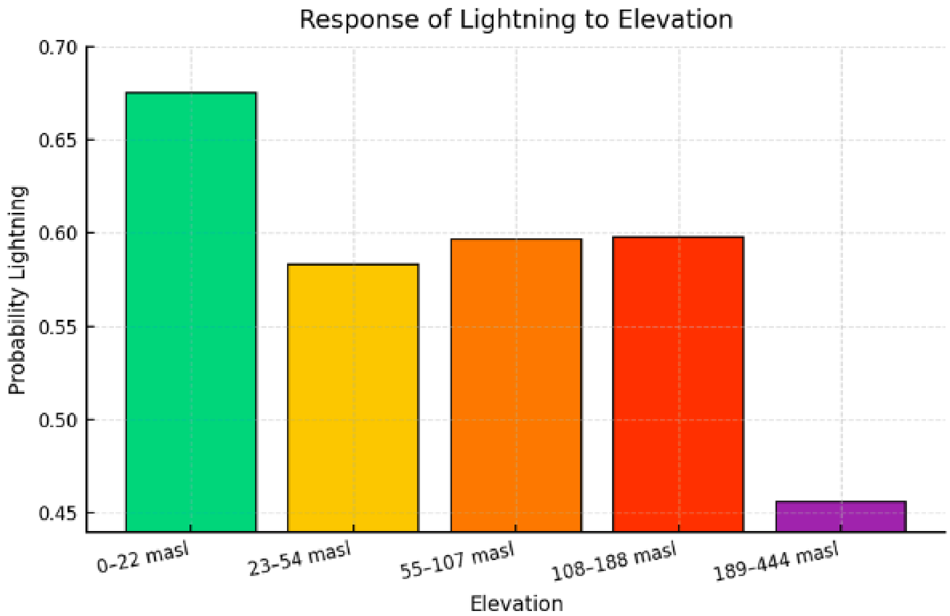

Figure 12: Effect of Elevation on Lightning Probability.

Figure 12 illustrates the relationship between lightning probability and elevation categories. The highest probability (~0.68) is observed at low elevations (0–22 masl), followed by the categories 55–107 masl and 108–188 masl, both showing similar values (~0.60). The mid-elevation range (23–54 masl) is slightly lower (~0.58). In contrast, the highest elevation class (189–444 masl) exhibits the lowest probability (~0.46). These results suggest that lightning is more frequent in lowland and foothill areas, whereas mountainous regions are less prone due to weaker convective activity.

In more detail, this pattern reveals a decreasing tendency of lightning occurrence with increasing altitude. Lowland areas are characterized by higher surface temperatures and abundant moisture, which enhance the formation of convective clouds that trigger lightning. On the other hand, mountainous regions are generally cooler and have more complex topography, which often suppresses convection and reduces lightning activity. This highlights the critical role of elevation in shaping the spatial distribution of lightning events.

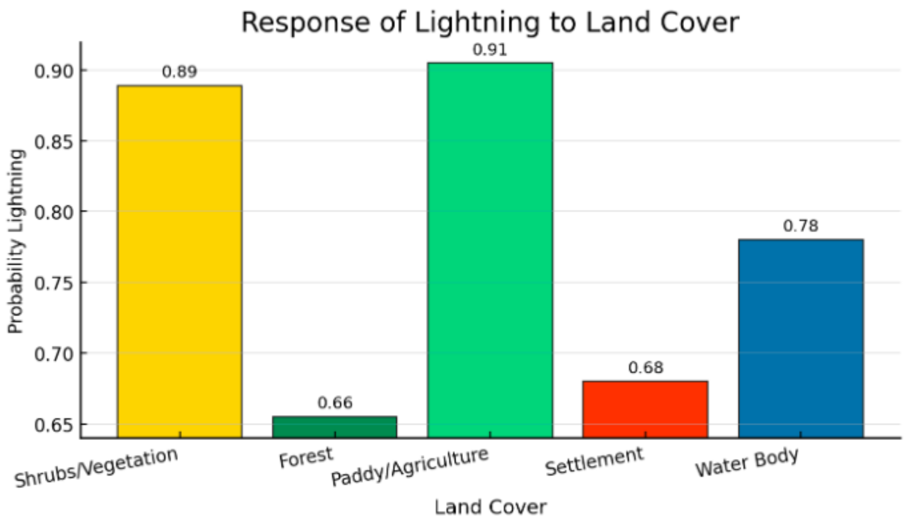

Figure 13: Influence of Land Cover on Lightning Events.

Figure 13 demonstrates the effect of land cover categories on lightning probability. Agricultural land (Paddy/Agriculture) records the highest probability (~0.91), followed by shrub/vegetation areas (~0.89). In contrast, forested areas exhibit the lowest probability (~0.66), while settlements show slightly higher values (~0.68). Water bodies fall within a moderate range (~0.78). These findings indicate that human-modified landscapes or sparsely vegetated areas are more vulnerable to lightning, whereas dense forests mitigate the risk through canopy shielding and microclimate moderation.

More specifically, the high lightning probability in agricultural and shrub-covered areas underscores the role of open landscapes with strong evapotranspiration in triggering local convection. Moisture released from farmlands or low vegetation contributes to abundant water vapor, thereby increasing the likelihood of thunderstorm development. In contrast, dense forest cover stabilizes surface temperatures and reduces latent heat flux, creating less favorable conditions for convective processes and lightning occurrence.

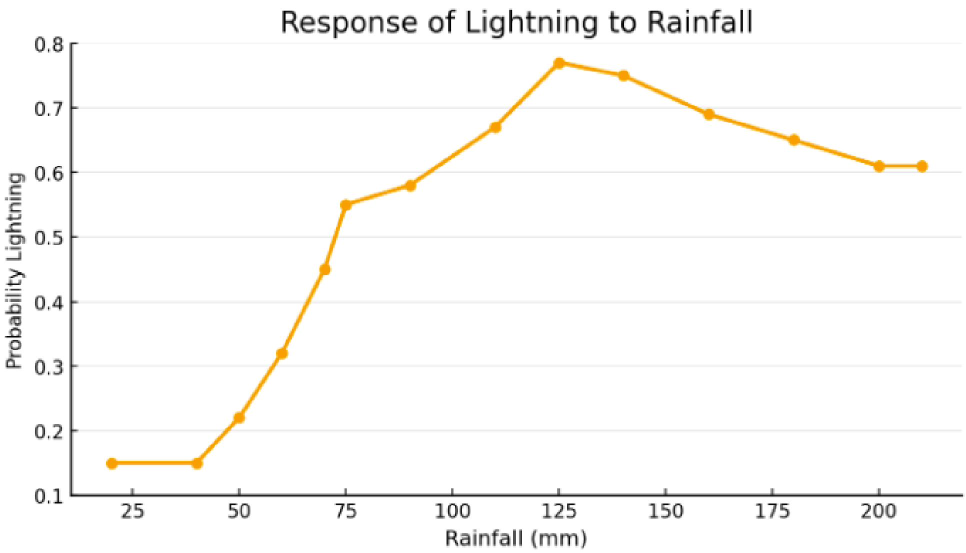

Figure 14: Response of Lightning Probability to Rainfall.

Figure 14 shows the response of lightning probability to monthly rainfall. At very low rainfall (20–30 mm), the probability remains minimal (~0.15), reflecting weak convective potential. As rainfall increases to around 60–80 mm, the probability rises steadily (~0.45–0.62), indicating strengthening convective activity. The curve continues to climb, reaching its maximum (~0.78) in the 120–140 mm range, which represents the optimal rainfall condition for lightning occurrence. Beyond this point, the probability gradually declines—dropping to ~0.70 at 160 mm and ~0.60 at >200 mm—suggesting that excessive rainfall tends to reduce lightning probability. This decline may be linked to the transition from convective to more stratiform rainfall processes, where cloud electrification becomes less efficient. Overall, the graph highlights a clear nonlinear relationship: lightning is most likely under moderate to high rainfall conditions, but not under extremely dry or excessively wet conditions.

This pattern indicates that rainfall acts as a regulator of atmospheric energy availability for lightning formation. Moderate rainfall enhances updraft strength and cloud electrification, favoring lightning, while extreme rainfall may be dominated by stratiform processes that suppress charge separation. The peak at 120–140 mm thus represents the balance point between sufficient moisture supply and optimal convective dynamics, making it the most favorable range for lightning activity.

Table 1. Relative contribution and permutation importance of predictor variables in the Maxent model.

Variable	Percent contribution (%)	Permutation importance (%)
Rainfall	79.1	89.3
Land Cover	12.1	7.9
Elevation	8.8	2.8

The impact of each predictive factor on the Maxent model was also assessed (Table 1). The findings reveal that precipitation was clearly the most significant factor, accounting for 79.1% of the model and exhibiting the greatest permutation importance (89.3%). This substantial influence validates that precipitation patterns are extremely important in determining where lightning strikes occur within the region under investigation.

Meanwhile, land cover accounted for 12.1% of the contribution and 7.9% of the permutation importance, suggesting a moderate but still relevant influence, likely reflecting the effect of surface characteristics on convection and thunderstorm development. Elevation, on the other hand, had the lowest contribution (8.8%) and permutation importance (2.8%), indicating that topographic variation exerts only a minor role compared to rainfall. In conclusion, the research underscores the significance of weather-related elements, notably precipitation levels, as the key environmental elements influencing the incidence of lightning strikes within this specific geographical area.

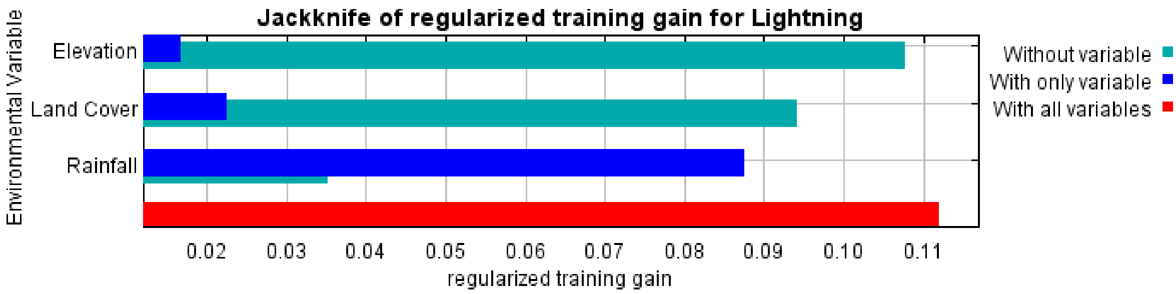

Figure 15: Jackknife of Regularized Training Gain.

Figure 15 presents the results of the Jackknife test, which evaluates the relative importance of each environmental predictor. When used in isolation (*with only variable*), Rainfall achieves the highest regularized training gain of about 0.09, making it the strongest single predictor of lightning distribution. Land cover follows with a gain of around 0.08, while Elevation shows the lowest contribution at only about 0.015, confirming its weak independent predictive power.

The critical role of rainfall is further evident when this variable is excluded (*without variable*). Removing rainfall causes the model's gain to drop from about 0.105 (with all variables) to nearly 0.02, representing the largest performance decrease. In contrast, excluding Elevation reduces the gain only slightly, from about 0.105 to 0.095, highlighting its marginal influence. Excluding land cover leads to a moderate decrease, indicating that it provides complementary but less unique information compared to rainfall. Overall, while the combined model (gain ≈ 0.105) delivers the best predictive performance, this analysis demonstrates that lightning distribution in Karimun Regency is primarily driven by rainfall (~0.09 gain), with secondary contributions from land cover (~0.08), and only negligible input from elevation (~0.015).

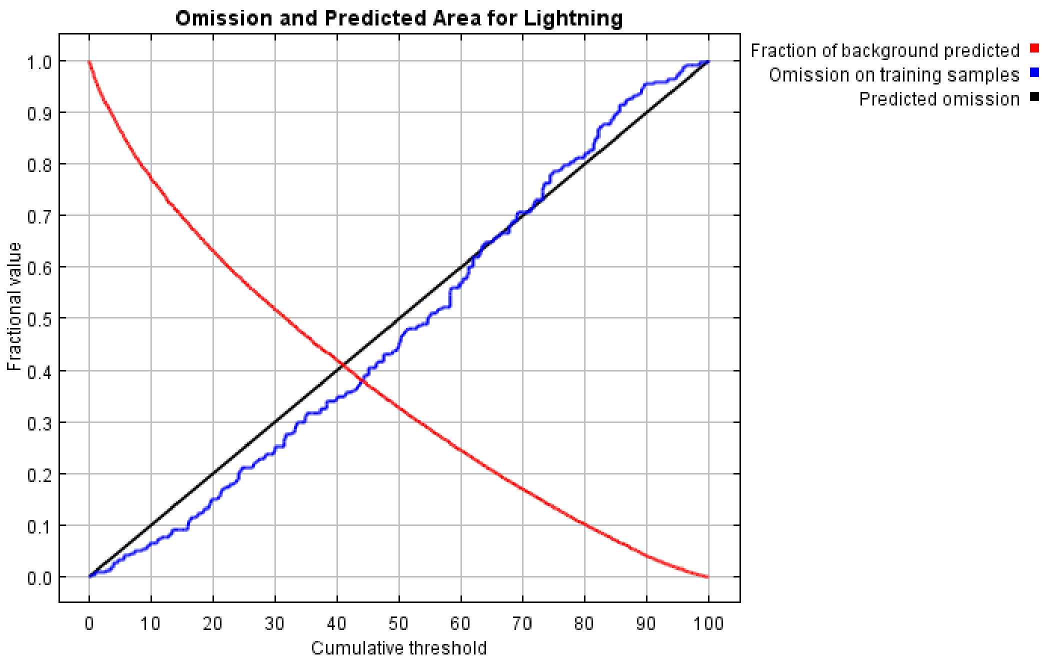

Figure 16: Omission Rate and Predicted Area Curve.

Figure 16 presents the omission and predicted area analysis. At low thresholds (0–20), the fraction of background predicted remains high, with about 78% at threshold 10 and 63% at threshold 20, while omission rates are relatively low (6.7%–15.5%). As the threshold increases, the predicted area decreases sharply, dropping to 42% at threshold 40 and 25% at threshold 60, whereas omission rises significantly to 36.7%–57.5%. At high thresholds (80–100), the predicted area becomes very small (≤10.9%) while omission approaches complete exclusion (81.8%–100%).

This pattern reflects a clear trade-off between spatial coverage and predictive accuracy. Lower thresholds yield broad predictions with higher sensitivity, suitable for early warning applications, while higher thresholds generate more confined predictions with greater specificity, useful for local-scale planning. The omission curve (blue) closely follows the expected omission line (black diagonal), with a maximum deviation of about 4.5%, confirming that the model is well-calibrated and provides reliable insights into lightning risk zones at different operational scales.

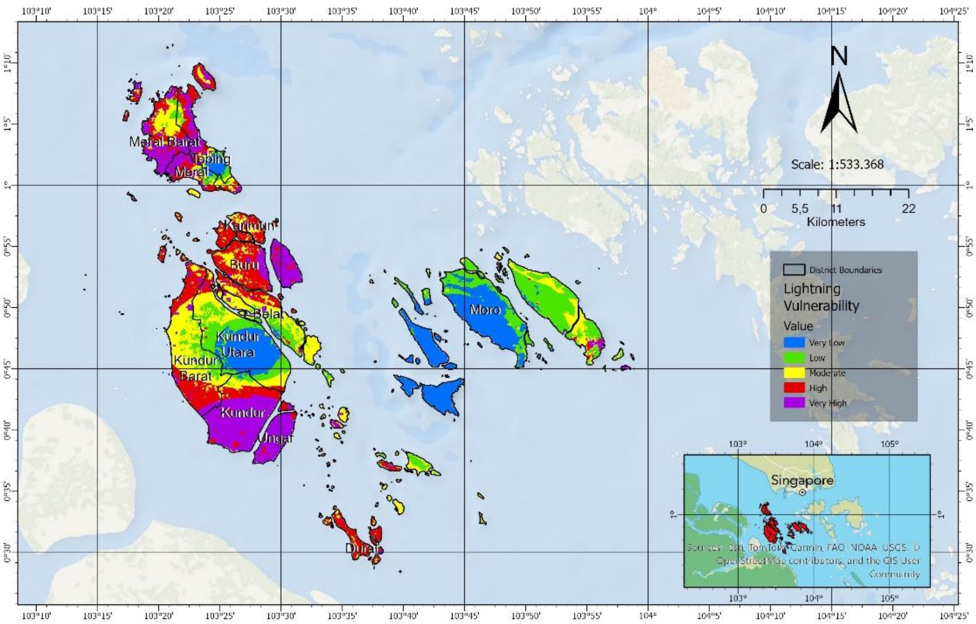

Figure 16: Lightning Vulnerability Map of Karimun Regency Based on MaxEnt.

As presented in Figure 16, the MaxEnt model mapped lightning vulnerability across the study area. The classification was divided into five levels, ranging from very low (areas least exposed) to very high (zones most at risk), with the intermediate categories being low, moderate, and high. The map reveals that the highest vulnerability zones (purple and red) are concentrated in Karimun, Buru, Kundur, Kundur Utara, Kundur Barat, as well as parts of Meral and Tebing, highlighting these districts as particularly prone to lightning events. In contrast, Moro Island shows extensive low to very low vulnerability (green and blue), especially in its central and eastern parts, while moderate zones (yellow) occur as transition areas in Belat and the eastern margins of Moro.

This spatial pattern reflects the combined influence of rainfall intensity, elevation, and land cover on lightning occurrence, as identified in the MaxEnt modelling results. The gradient from high to low vulnerability across different islands demonstrates clear spatial contrasts, which are critical for disaster risk management. The map therefore provides a practical tool for local authorities to prioritize high-risk districts such as Kundur and Karimun for mitigation measures, while ensuring that relatively safer regions like Moro are not overlooked in long-term planning for lightning hazard resilience.

Conclusion and Recommendation

This study reveals that lightning activity in Karimun Regency is primarily driven by environmental factors, with rainfall having the greatest influence on lightning occurrences. The predictive capability of the MaxEnt model was reflected in its AUC score of 0.654, where rainfall accounted for 79.1%, land cover for 12.1%, and elevation for 8.8%. Spatial analysis indicates that lowland areas (0–22 meters above sea level) experience the highest frequency of lightning strikes, particularly in regions dominated by shrub/vegetation. Despite a weak correlation between total monthly rainfall and lightning occurrences, the model highlights the significant role of land cover and elevation in shaping lightning distribution. The findings suggest that future mitigation strategies should prioritize high-risk lowland areas, particularly during the afternoon when lightning activity peaks. Further model refinement with meteorological variables such as CAPE could enhance prediction accuracy. Additionally, protection measures should be focused on areas with dense vegetation, and regional planners should consider incorporating lightning hazard data into zoning and infrastructure design.

Acknowledgment

The author is deeply grateful to the Indonesian Agency for Meteorology, Climatology, and Geophysics (BMKG) for the scholarship that made this research possible. The author also extends sincere thanks to the Hang Nadim Meteorological Station Class I Batam for providing critical lightning data and to the Raja Haji Abdullah Meteorological Station Class IV Karimun for supplying rainfall data. The financial and data contributions from these institutions were essential to the success of this study.

References

Albrecht, R. I., Goodman, S. J., Buechler, D. E., Blakeslee, R. J., & Christian, H. J. (2016). Where are the lightning hotspots on earth? *Bulletin of the American Meteorological Society*, *97*(11), 2051–2068. https://doi.org/10.1175/BAMS-D-14-00193.1

Aldrian, E., & Dwi Susanto, R. (2003). Identification of three dominant rainfall regions within Indonesia and their relationship to sea surface temperature. *International Journal of Climatology*, *23*(12), 1435–1452. https://doi.org/10.1002/joc.950

Bourscheidt, V., Pinto, O., Naccarato, K. P., & Pinto, I. R. C. A. (2009). The influence of topography on the cloud-to-ground lightning density in South Brazil. *Atmospheric Research*, *91*(2–4), 508–513. https://doi.org/10.1016/j.atmosres.2008.06.010

Chen, F., Du, Y., Niu, S., & Zhao, J. (2015). Modeling forest lightning fire occurrence in the Daxinganling Mountains of Northeastern China with MAXENT. *Forests*, *6*(5), 1422–1438. https://doi.org/10.3390/f6051422

Christian, H. J., Blakeslee, R. J., Boccippio, D. J., Boeck, W. L., Buechler, D. E., Driscoll, K. T., Goodman, S. J., Hall, J. M., Koshak, W. J., Mach, D. M., & Stewart, M. F. (2003). Global frequency and distribution of lightning as observed from space by the Optical Transient Detector. *Journal of Geophysical Research: Atmospheres*, *108*(1). https://doi.org/10.1029/2002jd002347

Cummins, K. L., & Murphy, M. J. (2009). An overview of lightning locating systems: History, techniques, and data uses, with an in-depth look at the U.S. NLDN. *IEEE Transactions on Electromagnetic Compatibility*, *51*(3 PART 1), 499–518. https://doi.org/10.1109/TEMC.2009.2023450

Elith, J., Phillips, S. J., Hastie, T., Dudík, M., Chee, Y. E., & Yates, C. J. (2011). A statistical explanation of MaxEnt for ecologists. *Diversity and Distributions*, *17*(1), 43–57. https://doi.org/10.1111/j.1472-4642.2010.00725.x

Fuchs, B. R., & Rutledge, S. A. (2018). Investigation of Lightning Flash Locations in Isolated Convection Using LMA Observations. *Journal of Geophysical Research: Atmospheres*, *123*(11), 6158–6174. https://doi.org/10.1002/2017JD027569

Fuchs, B. R., Rutledge, S. A., Bruning, E. C., Pierce, J. R., Kodros, J. K., Lang, T. J., MacGorman, D. R., Krehbiel, P. R., & Rison, W. (2015). Environmental controls on storm intensity and charge structure in multiple regions of the continental United States. *Journal of Geophysical Research*, *120*(13), 6575–6596. https://doi.org/10.1002/2015JD023271

Journal of Geophysical Research Atmospheres - 1998 - Petersen - On the relationship between cloud-to-ground lightning and.pdf. (n.d.).

Mori, S., Jun-Ichi, H., Tauhid, Y. I., Yamanaka, M. D., Okamoto, N., Murata, F., Sakurai, N., Hashiguchi, H., & Sribimawati, T. (2004). Diurnal land-sea rainfall peak migration over Sumatera Island, Indonesian Maritime Continent, observed by TRMM satellite and intensive rawinsonde soundings. *Monthly Weather Review*, *132*(8), 2021–2039. https://doi.org/10.1175/1520-0493(2004)132<2021:DLRPMO>2.0.CO;2

Peterson, M., Mach, D., & Buechler, D. (2021). A Global LIS/OTD Climatology of Lightning Flash Extent Density. *Journal of Geophysical Research: Atmospheres*, *126*(8). https://doi.org/10.1029/2020JD033885

Phillips, S. B., Aneja, V. P., Kang, D., & Arya, S. P. (2006). Modelling and analysis of the atmospheric nitrogen deposition in North Carolina. *International Journal of Global Environmental Issues*, *6*(2–3), 231–252. https://doi.org/10.1016/j.ecolmodel.2005.03.026

Pineda, N., Rigo, T., Bech, J., & Soler, X. (2007). Lightning and precipitation relationship in summer thunderstorms: Case studies in the North Western Mediterranean region. *Atmospheric Research*, *85*(2), 159–170. https://doi.org/10.1016/j.atmosres.2006.12.004

Rakov, V. A., & Uman, M. A. (2001). *Lightning*.

Santos, A. P. P. dos, Ferreira, D. B. da S., Nascimento Júnior, W. da R., Souza-Filho, P. W. M. e., Pinto Júnior, O., Lima, F. J. L. de, Bourscheidt, V., Mattos, E. V., Costa, C. P. W. da, Nogueira Neto, A. V., & Tedeschi, R. G. (2024). Lightning under Different Land Use and Cover, and the Influence of Topography in the Carajás Mineral Province, Eastern Amazon. *Atmosphere*, *15*(3). https://doi.org/10.3390/atmos15030375

Williams, E. R. (2005). Lightning and climate: A review. *Atmospheric Research*, *76*(1–4), 272–287. https://doi.org/10.1016/j.atmosres.2004.11.014

Williams, E., & Stanfill, S. (2002). The physical origin of the land-ocean contrast in lightning activity. *Comptes Rendus Physique*, *3*(10), 1277–1292. https://doi.org/10.1016/S1631-0705(02)01407-X

Yusnaini, H., Marzuki, Muharsyah, R., Vonnisa, M., & Tangang, F. (2021). Influence of topography on lightning density in Sumatra. *Journal of Physics: Conference Series*, *1876*(1). https://doi.org/10.1088/1742-6596/1876/1/012022